World Conference on Timber Engineering Oslo 2023

GLUED-LAMINATED TIMBER UNDER EXTREME COLD TEMPERATURES SUBJECTED TO IMPACT LOADING

Nicole Wight[1], Christian Viau[2], Patrick Heffernan[3]

ABSTRACT: With the increasing turbulence in the global security environment, comes the requirement for an increasing presence in the Canadian Arctic to respond to regional challenges and provide security. Such presence requires temporary and permanent installations, which must inherently carry with it some considerations for extreme load events, such as blast and impacts. In tandem with this is the expanding need to build more environmentally sustainable buildings, for which wood has been identified in recent years. However, questions remain on how wood responds to blast and impact loads when exposed to cold temperatures, typical of the arctic region. To respond to this gap in research, an experimental program was carried out to investigate the flexural behaviour of glued-laminated timber (glulam) subjected to impact loading under ambient and winter arctic temperatures. Dynamic testing was conducted using a drop weight impact hammer. For strain rates between 1.13 to 1.38 s^{-1}, an average dynamic increase factor of 1.23 on the maximum resistance at ambient temperatures was observed. The cold temperature beams were seen to experience a 13% increase in strength beyond their normal temperature counterparts under dynamic effects. Increases in stiffness due to cold temperature were also observed under static and dynamic loading.

KEYWORDS: Impact, Glulam, Arctic, Strain Rate, Cold Temperature, Dynamic Increase Factor

1 INTRODUCTION

In recent decades, there has been an upward trend in infrastructure and buildings being exposed to blast and impact loading, as well as an increased use of wood as a construction material for mid- and high-rise timber and timber-hybrid structures. However, despite wood being mentioned in blast design standards [1, 2], current provisions are lacking in quantity and extent, due to them being based on limited early research on light-frame wood shelters [3]. The exposure of structural materials to high strain rates typically leads to increases in strength and, in some cases, stiffness, generally quantified using a dynamic increase factor (DIF). Shock tube testing, which simulates the effects of far-field blast explosions, has been used to determine DIF values for various wood elements under normal temperature, most notably glued-laminated timber (glulam) and cross-laminated timber (CLT), where DIFs of 1.14 and 1.28, respectively, have been reported [4, 5]. Other studies investigating the behaviour of light-frame wood systems [6-9] and timber connections under high strain-rates [10-12] have also been conducted.

Various countries, including Canada and allies, have a vested interest in asserting sovereignty in their Northern regions, and the need to have an active and visible presence in these cold environments has become incredibly prevalent with the current global security environment [13]. Canadian Forces Station (CFS) Alert, located 817 km from the geographic North Pole, represents not only the most northerly permanently inhabited place in Canada, but also in the world, where during the winter months the average daily temperature is -40 °C [14]. As such, materials capable of withstanding these temperatures without adverse effects on their mechanical properties and durability are critical to expanding infrastructure in Northern Regions of Canada. Already, large infrastructure constructed with engineered wood products are being developed for use in colder regions of Canada. For example, the Macaisagi Bridge in northern Quebec, Canada, built in 2011 out of CLT and glulam with a 1,790 kN capacity, spans 68 m and experiences temperatures as low as -45 °C [15]. Understanding how extreme cold temperatures affect a material's mechanical properties is required to provide users with safe, durable, and effective designs. Despite its application in cold weather regions, little research has been conducted on the performance of glulam under arctic conditions, none of which examined static or dynamic bending strength [15-17].

Beirnes et al. investigated the impact resistance of thin ultra-high performance fibre reinforced concrete (UHPFRC) panels under extreme cold temperatures. An increase in the static strength and an increase in the panel residual strength under impact loading of the cold panels compared to their ambient temperature counterparts was observed [18]. No additional studies investigating the effects of cold temperature on the impact or blast resistance of structures could be found.

[1] Nicole Wight, Force Protection Engineer Officer, 1 Engineer Support Unit, Canadian Armed Forces, Canada, nicole.wight@forces.gc.ca

[2] Christian Viau, Assistant Professor, Department of Civil and Environmental Engineering, Carleton University, Canada, christian.viau@carleton.ca

[3] Patrick Heffernan, Professor, Department of Civil Engineering, Royal Military College of Canada, Canada, Pat.Heffernan@rmc.ca

https://doi.org/10.52202/069179-0041

Canada's Blast Design Standard, CSA S850, currently provides a DIF value for glulam of 1.4 under flexural loading [1], a value which has been reported to be nonconservative by recent studies on glulam [4, 19]. In addition, current blast design standards do not account for the cold weather behaviour of materials under blast loading [1, 2]. To address this gap in research, the below experimental program investigated the effect of extreme cold temperature on the mechanical strength properties of glulam under both quasi-static and high-strain rates for the purpose of expanding glulam's use in structures under extreme cold temperatures.

2 EXPERIMENTAL PROGRAM

2.1 DESCRIPTION OF TEST SPECIMENS

A total of fifteen 137 mm x 178 mm x 1650 mm NordicLam+ 24F-ES grade glulam beams were tested under quasi-static and dynamic loading, at both ambient and extreme cold temperatures, to document high strain-rate effects and their behaviour under impact loading conditions. As previous research has indicated that finger joints may affect the failure of beams under high strain rates, beams of multilaminate widths were chosen to minimise this effect [4]. For all specimens presented in this paper, the prefix "S" refers to a specimen that was tested quasi-statically, while the prefix "D" refers to a specimen that was tested dynamically. Similarly, this was followed by the letter "A" or "C", indicating that the specimen was tested at ambient temperature or cold temperature, respectively.

2.2 TEMPERATURE MONITORING

All cold specimens were placed into a cold temperature freezer at -70 °C for a minimum of seven days prior to testing. All beams were equipped with a Type T thermocouple adhered to their side approximately 8 cm from the centreline in order to record the beam's surface temperature. In order to assess internal temperatures of the specimens, a test beam was placed in the cold temperature freezer with thermocouples installed at depths of 63 mm, 42 mm, 21 mm, and on the surface. The readings obtained from the test beam were then used to develop a relationship between the surface and internal temperatures. Using this information to develop a correlative relationship, the time to required for the beams to reach an internal temperature of -70 °C and the beams' internal temperatures at the time of testing could be determined.

2.3 STATIC TESTING

Quasi-static four point bending flexural tests were conducted on seven of the fifteen specimens to serve as a baseline with which to compare the dynamic results. The quasi-static test setup can be seen in Figure 1. These tests, adapted from ASTM D198 [20], resulted in the quasi-static flexural strength values that were normalised to a standardized 1-minute load duration, as outlined in Section 3.2. A linear variable differential transformer (LVDT) connected at the beam's midspan recorded the beam's displacement, while two strain gauges positioned on the tension side of the beam and two on the compression side of the beam at midspan measured the specimens' strain deformations. A load cell within the hydraulic head measured the applied force, and applied a load at a displacement-controlled rate of 1 mm/min. This resulted in an average time to failure of 15.2 mins for the small normal temperature beams and 13.4 mins for the cold temperature beams. Simply supported boundary conditions were provided using the same rollers and load transfer bar used for the dynamic tests. A clear span of 1,479 mm was used throughout testing, with the load being applied at the beam third points. This allowed for an area of constant moment and zero shear force in the central third of the beam. To avoid crushing, 150 mm long plates at the load-application points and beam ends were used.

Figure 1: *Static test setup*

2.4 DYNAMIC TESTING

Dynamic testing was conducted using the newly established drop weight impact testing facility at the Royal Military College of Canada (Kingston, ON Canada), capable of imparting up to 23 kJ of energy onto small- to full-scale structural elements. The impact hammer consists of a weighted box that travels along six-meter-tall rails using six pillow block ball bearings to guide the box. All ambient temperature dynamic beams were subject to an 1800 mm drop with a weight of 141.7 kg and all cold temperature beams were subject to a 2000 mm drop with a weight of 141.7 kg. The dynamic test set-up can be seen in Figure 2. A data acquisition system capable of recording up to 500 kHz was used. An electromagnet was used to raise the box to the required

https://doi.org/10.52202/069179-0041

drop height, which was determined using a linear encoder attached to the drop weight. The linear encoder also permitted for the box kinematics at impact to be determined.

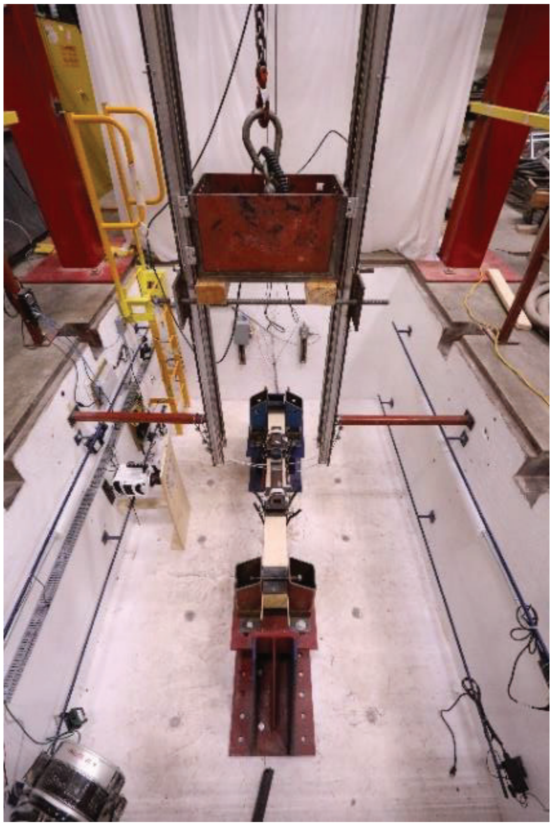

Figure 2: *Dynamic test setup*

Support rollers identical to those in the static test setup were utilized, facilitating the comparison between both sets of tests. Lateral supports were provided at the beam ends to minimize the likelihood of lateral beam instability during response. Additionally, brace plates were placed on top of the beam at each end to prevent upward motion of the beam after initial impact. A load transfer beam was used to distribute the impact load across the central third of the beam in order to create an area of constant moment and zero shear force. The beams were instrumented with piezoelectric force sensors under each support and under the load application points in order to determine the support reactions and the applied load. The beam's displacement-time history was recorded using both a laser and a string potentiometer, while two strain gauges positioned on the tension side of the beam and two on the compression side of the beam at midspan measured the specimens' strains. Three high speed cameras, capturing images at 10,000 fps, 1,000 fps and 500 fps, were used to record the beam's behaviour and potential failure locations.

3 EXPERIMENTAL RESULTS

3.1 TEMPERATURE MONITORING

Specimen SC3 was prepared in the manner outlined in Section 2.2. Upon conditioning, SC3 was removed from the freezer and the change in internal temperature was monitored over time. The output of this test allowed for the temperature time curves to be used to relate the internal temperatures to those of the various tests. The average rate of warming in the beam across the four thermocouple depths was 0.72 °C/min. The surface thermocouple temperatures recorded during the tests were also compared to the values obtained by the test beam and good agreement was observed. As a result, the average internal temperature for all static beams was -46.8 °C at the midpoint of testing and -43.5 °C at failure. Due to the short duration of testing, the average internal temperature for all dynamic beams was -47.1 °C at failure. In all cases, these temperatures are within the range of temperatures experienced in the Arctic.

3.2 STATIC TESTING RESULTS

Failure was established to be the point during testing where the specimen experienced a sudden drop in load and could no longer support additional load. The stiffness was taken as the slope of the resistance displacement curve from 40% to 90% of the beam's ultimate capacity. The failure load for each beam was normalized to a 100% strength value corresponding to a testing time of 1 minute in order to normalise all static results using Equation (1) [21].

$$SL = 100.0 - 3.5Log_{10}T_r \quad (1)$$

where SL = stress level factor in the beam and T_r = time to failure in minutes.

The results from the normal and cold temperature static tests are summarized in Table 1, including the static maximum resistance ($R_{s,max}$), stiffness (K), strain rate ($\dot{\epsilon}$), the time-to-failure and whether the beam failed in flexure, shear, or combined flexure and shear.

The average peak resistance for the normalized static normal temperature tests was 185.6 kN with a coefficient of variation (COV) of 0.12. From the results, it can be observed that some of the beams failed in flexure, while others failed in shear. Before testing, the beams' capacities were checked for governing failure mode, and the shear failure capacity of the beams was determined to not govern the design of the specimens. When only the beams that failed purely in bending were considered, the peak resistance was 166.3 kN with a COV of 0.02. The average stiffness for the normalized static normal temperature tests was 11,900 kN/m with a COV of 0.02. As would be expected, when only the bending failures are considered, the stiffness does not change dramatically, with the average stiffness being 11,670 kN/m with a COV of 0.01. The average surface temperature of the normal temperature beams was 19.7 °C during testing.

https://doi.org/10.52202/069179-0041

Table 1: Static test results

Sample	$R_{s,max}$	K	$\dot{\varepsilon}$ (x10^{-6})	Time to Failure	Failure Mode
	kN	kN/m	s^{-1}	mins	
Normal Temperature Beams					
SN1	163.4	11,490	5.48	13.3	Flexure
SN2	190.0	12,250	4.74	13.6	Shear
SN3	169.3	11,840	4.98	14.6	Flexure
SN4	219.6	12,020	5.08	19.3	Shear
Avg	185.6	11,900	5.07	15.2	
Std Dev	22.0	275	2.64	2.4	
COV	0.12	0.02	0.05	0.16	
Cold Temperature Beams					
SC1	182.9	13,760	6.44	13.0	Flexure
SC2	189.8	13,800	4.95	13.4	Shear
SC3	155.0	13,950	4.99	10.9	Flexure
Avg	175.9	13,840	5.46	12.4	
Std Dev	15.1	79	0.70	1.1	
COV	0.09	0.01	0.13	0.09	

The average peak resistance for all normalized static cold temperature tests was 175.9 kN with a COV of 0.09. When only the beams that failed purely in bending were considered, the peak resistance was 168.9 kN with a COV of 0.08. The average stiffness for all normalized static cold temperature tests was 13,840 kN/m with a COV of 0.01. As would be expected, when only the bending failures are considered, the stiffness does not change dramatically, with the average stiffness being 13,850 kN/m with a COV of 0.01. The average internal temperature of the cold temperature beams at failure was -43.5 °C and the average surface temperature at failure was -39.9 °C.

3.3 DYNAMIC TESTING

Dynamic failure of the beam specimens was determined to occur at the peak resistance, consistently followed by a sudden drop in resistance. Unlike static loading, the dynamic resistance of a beam cannot be obtained by the simple summation of the reactions as this will not give an accurate reflection of the beam's response. This is due to the dynamic resistance being dependant not only on the dynamic reactions, but also the boundary conditions, whether the element response is elastic or inelastic, and the applied load [22]. The dynamic resistance was obtained using Equations (2) and (3), where the latter was used in order to account for the distributed mass of the beam and the point loads of the load transfer beam. Further information on the derivation of these expressions can be found in [22, 23].

$$R(t) = \frac{6}{L}\left[V(t) \times x_{eq} + 0.5 \times \left(\frac{L}{3} - x_{eq}\right) \times F(t)\right] \tag{2}$$

$$x_{eq} = \frac{0.102\bar{m} \times L^2 + 0.290m_c \times L}{0.319\bar{m} \times L + 0.870m_c} \tag{3}$$

where $R(t)$ = beam dynamic resistance, $V(t)$ = dynamic reaction, $F(t)$ = applied force, L = beam clear span, x_{eq} = distance from the support to the point of application of the equivalent inertia force, $\bar{m}$ = the distributed mass of the beam and m_c = half of the mass of the load transfer beam lumped at the load application points.

Similar to the static tests, the initial beam stiffness was taken as the slope of the resistance displacement curve from 40% to 90% of the beam's ultimate capacity. The results from the dynamic tests for normal and cold temperature beams can be seen in Table 2, including the dynamic maximum resistance ($R_{d,max}$), stiffness (K), strain rate ($\dot{\varepsilon}$), duration of load and whether the beam failed in flexure, or shear.

Table 2: Dynamic test results

Sample	$R_{d,max}$	K	$\dot{\varepsilon}$	Duration of Load	Failure Mode
	kN	kN/m	s^{-1}	ms	
Normal Temperature Beams					
DN1	210.7	12,890	1.36	9.5	Flexure
DN2	207.7	16,140	1.13	10.0	Flexure
DN3	190.3	14,340	1.38	9.6	Flexure
DN4	208.9	15,410	1.33	9.4	Flexure
Avg	204.4	14,700	1.30	9.6	
Std Dev	8.2	1,220	0.10	0.2	
COV	0.04	0.08	0.08	0.02	
Cold Temperature Beams					
DC1	226.8	16,500	1.25	8.9	Shear
DC2	226.0	17,640	1.28	9.1	Flexure
DC3	229.2	16,700	1.14	10.0	Flexure
DC4	239.4	17,360	1.31	10.3	Flexure
Avg	230.3	17,050	1.25	9.6	
Std Dev	5.4	465	0.06	0.6	
COV	0.02	0.03	0.05	0.06	

For strain rates between 1.13 to 1.38 s^{-1}, the average dynamic peak resistance for the normal temperature beams was 204.4 kN with a COV of 0.04. The average stiffness for the normal temperature beams was 14,700 kN/m with a COV of 0.08.

All but one dynamic cold temperature beam failed in flexure, with specimen DC1 failing in shear. For strain rates between 1.14 to 1.31 s^{-1}, the average dynamic failure resistance for the cold temperature beams was 230.3 kN with a COV of 0.02. The average stiffness for the cold temperature beams was 17,050 kN/m with a COV of 0.03. If only the flexural failures are considered, the average dynamic failure resistance for the cold temperature beams was 231.5 kN with a coefficient of variation (COV) of 0.02. The average stiffness for the cold temperature beams was 17,236 kN/m with a COV of 0.02. As can be seen from these values, the beam that failed in shear, had very similar failure values to the other beams and as such the results do not differ greatly when this beam's data is omitted.

3.4 FAILURE MODES

All specimens behaved in a linear elastic manner and failed in a brittle manner via tensile failure initiated at a knot or natural defect. Some specimens failed in shear or combined flexural and shear. One potential cause is the presence, or lack, of defects in the central third of the beam, where the bending moment is constant and at its maximum. In all cases of flexural failure, this was identified as having been initiated at a knot or natural defect in the beam. However, in all specimens that failed in shear, no visible natural defects, or knots on the tensile outer edge of the beams within the central third could be identified. This caused a shift in governing failure mode to a shear dominated failure mode, rather than flexural as initiated on the bottom tension-side fibres. While specimens without defects were not specifically chosen for this study, the beams were limited in size due to the geometrical constraints of the cold temperature freezer, whereas beams used in construction would likely be significantly greater in size, largely guaranteeing that defects would always be present.
Static normal temperature specimens consistently had more prominent crack dimensions than their cold temperature counterparts. Images of a representative failure of a specimen under static loading is shown in Figure 3. The failure in both the normal temperature and cold temperature beams, occurred at a knot or natural defect, and both exhibited a similar crack pattern.

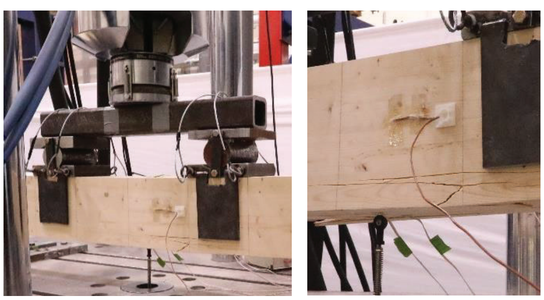

(a) *Global view* ***(b)*** *Close-up view*

Figure 3: *Failure of static normal temperature specimen SN3*

Figure 4 and Figure 5 show still images taken from one of the high-speed cameras of specimens DN4 and DC4, respectively, immediately following failure. It can be seen that the crack pattern in the normal temperature beam is more apparent that the crack pattern in the cold temperature beam. Both dynamic specimens, when viewing the beams after testing, had similar crack propagation patterns to the statically tested specimens.

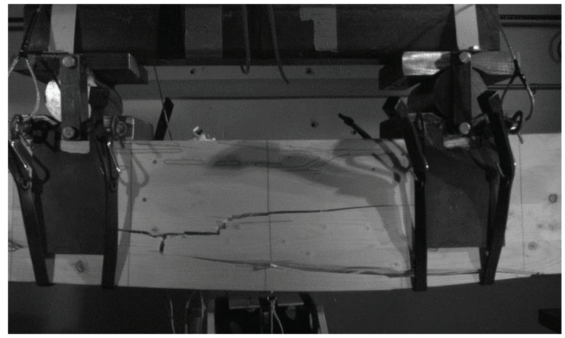

Figure 4: *Failure of dynamic normal temperature specimen DN4*

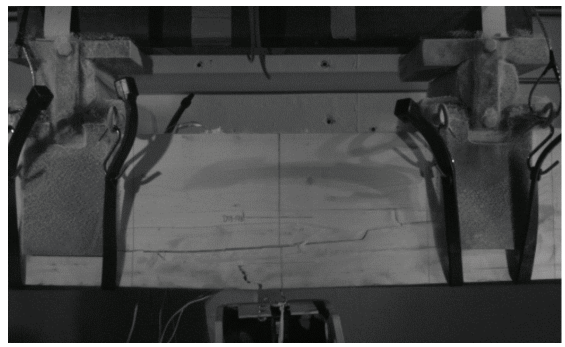

Figure 5: *Failure of dynamic cold temperature specimen DC4*

4 HIGH STRAIN RATE AND COLD EFFECTS

For the analysis presented below, inferences regarding the experimental test results must be limited to specimens with identical failure modes. It is for this reason that all specimens which failed in shear were not considered when determining the DIF for the resistance and stiffness. Representative resistance curves from the static and dynamic testing can be seen in Figure 6. In each resistance curve, the point at which failure occurred, based on the maximum resistance, is denoted with an 'x'. Here the trends in the data can be visually observed.
No increase in strength between the normal and cold temperature static tests is observed; however, it can be seen that the cold temperature specimens seem to experience an increase in stiffness.
The dynamic resistance curves can be seen to have more fluctuation, likely caused by dynamics of the system, or more specifically the vibrations that occur within a dynamic system, which is to be expected under impact loading. Earlier it was mentioned that 40-90% of the resistance curves were used in order to calculate the stiffness of the beams. The reasoning behind this is apparent when the curves are viewed. All dynamically tested beams exhibited a higher initial stiffness as the system settled, which was not representative of the remainder of the resistance curve. There is then a relatively constant second slope which was taken to be the beams actual response to the impact loading up until near failure. When looking at the dynamic resistance curves, it

https://doi.org/10.52202/069179-0041

can be seen that the dynamic specimens exhibited higher capacity and stiffness than their static counterparts, indicating the increase in strength and stiffness experienced by the glulam at high strain rates.

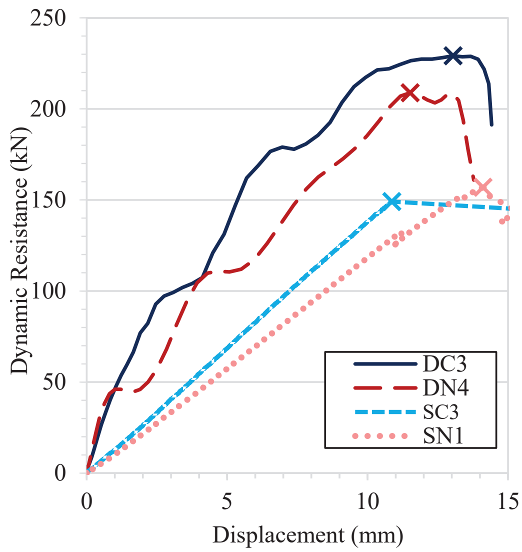

Figure 6: *Representative resistance curves*

The use of identical spans, boundary conditions, and loading conditions allowed for a direct comparison between the static and dynamic test results for the purpose of quantifying high strain-rate effects on the glulam specimens. The DIF on the peak resistance was calculated using Equation (4).

$$DIF = \frac{R_{d,max}}{R_{s,nor}} \tag{4}$$

where $R_{d,max}$ = maximum dynamic resistance and $R_{s,nor}$ = maximum static resistance normalized to a 100% strength value corresponding to a testing time of 1 minute based on Karacabeyli and Barrett [21].
The dynamic testing results, for strain rates in the range of 1.13 to 1.38 s^{-1}, revealed an increase in strength for both the ambient and cold temperature beams. For the normal temperature specimens, an average DIF of 1.23 on the normal temperature beam's peak resistance was determined when compared to the average static peak resistance. Looking at the current Canadian Blast Design Standard [1], a value of 1.4 is given, which is much higher than the value determined under normal temperature testing. For the cold temperature specimens, an average DIF of 1.37 was determined when compared to the average static cold temperature peak resistance. It is clear that high strain-rate effects are present within the cold specimens, and the preliminary results indicate that a higher DIF is attributable to cold temperature effects. A further number of tests are required to fully substantiate these effects. There is currently no stipulation for the performance of structures under cold temperatures in the current Canadian Blast Design Standard [1]. The observed DIFs can be visually seen in Figure 7, which summarises the obtained dynamic increase factors.

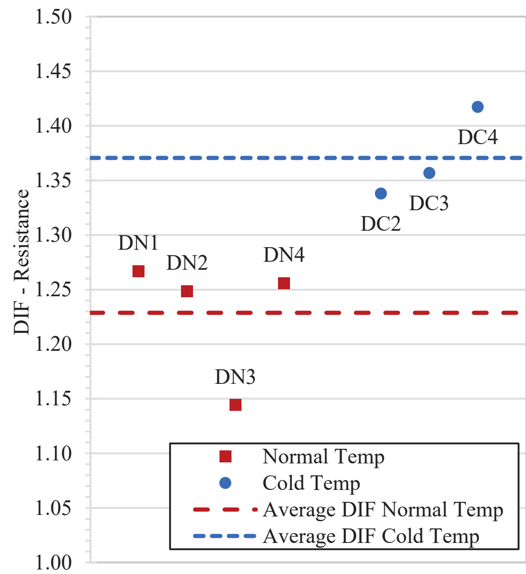

Figure 7: *Summary of observed DIFs*

Statistical analysis was done on each of these observations. It was found that the normal temperature beams dynamic to static resistance values were supported by statistical analysis using a T-Test with a 95% confidence interval. However, when looking at the cold temperature data the confidence interval that the results were statistically significant was only supported by a confidence interval of 85%. This was due to the smaller sample size, due to the omission of the specimens having failed in shear in the analysis. As such, it is recommended that further testing be done regarding the effects of cold under impact loading to further reinforce the observation that cold temperature beams under high strain rates exhibit an apparent increase in resistance when compared to their static cold temperature counterparts.
An increase in stiffness was observed when comparing the dynamic tests to their normal temperature counterparts. An average DIF on the modulus of elasticity of 1.26 and 1.24 on the beam's stiffness was determined for the normal and cold temperature specimens, respectively, when compared to their respective static tests. These observations were supported by statistical analyses by using a T-Test, with a confidence interval of 95%.
Cold temperature effects are summarized in Table 3 where cold temperature effects on the mechanical properties of glulam under static and dynamic loading were quantified.
In all cases, the normal and cold temperature values were juxtaposed against one another by comparing the static-to-static tests and dynamic-to-dynamic tests. These observations were supported by statistical analyses via T-Tests, with a confidence interval of 95%. Specifically, no cold temperature effects could be identified for the static resistance. Considering the dynamic tests, the cold temperature beams experience a 13% increase in strength compared to their normal temperature counterparts.

Table 3: *Effect of cold on strength and stiffness*

Comparison	Avg. Normal Temp. Value	Avg. Cold Temp. Value	Cold Factor
Static normal to cold temperature resistance (kN)	166.3	168.9	1.02
Static normal to cold temperature stiffness (kN/m)	11,670	13,850	1.19
Dynamic normal to cold temperature resistance (kN)	204.4	231.5	1.13
Dynamic normal to cold temperature stiffness (kN/m)	14,700	17,240	1.17

Previous research on clear wood found an 18% increase in bending strength at 4% moisture content on clear wood at -50 °C compared to 20 °C [24]. However, this testing was not on glulam but involved clear wood, which is void of defects and finger joints. As outlined in the above test results, the presence of defects highly influences the failure load of specimens. As such, the effects of cold temperature on the overall lignin matrix in the wood may be insignificant when compared to the effects of defects. No studies on the flexural behaviour of glulam under similar temperatures could be found.

One possible cause of this discrepancy between static and dynamic strengths amongst the cold temperature specimen is the effect of ice between the wood fibres. The ice content in the specimens from the inherent moisture content of the wood may alleviate and delay the initial growth of microcracks, resulting in a higher strength under short duration loading. When looking at the static tests, since the loading occurs under a much longer duration, microcrack growth is able to develop and not affect the beam strength over the significantly longer load duration. Additionally, the tested beams had a relatively low moisture content (on average 8.9%), which would have reduced the ice content, thereby reducing the effect that the water molecules would have on the behaviour of the glulam specimens.

In terms of initial stiffness, an apparent increase in stiffness observed in the cold temperature specimens under both static and dynamic testing when compared to their normal temperature counterparts could be observed. This observation is corroborated by previous studies, which studied different forms and types of wood at lower temperatures [16, 24-26]. This is likely due to the freezing of the water content within the beams and potentially the stiffening of the adhesive used. When looking at the static tests there was a 19% increase in stiffness observed. When looking at the dynamic tests, there was a 17% increase in stiffness observed. Both values are very close to one another, indicating a uniform increase in stiffness due to cold, regardless of the type of loading.

From a design perspective, cold temperature effects appear to improve the dynamic performance of glulam at cold temperatures. As such, if the structure is expected to remain at cold temperature for the duration of it's use and occupancy, then these potential strength increases could be considered. However, if the structure is expected to experience a wider range of temperatures, then cold temperature effects can conservatively be omitted for design purposes.

5 CONCLUSIONS

For a dynamic strain-rate range of 1.13 to 1.38 s^{-1}, a DIF of 1.23 on the maximum resistance at ambient temperatures was observed. An increase in strength of 13% in the cold temperature beams under dynamic loading was observed. The cold did not appear to influence the static resistance of the beams. Dynamic effects caused an increase in the stiffness, resulting in an average DIF on the stiffness of 1.25 for both the normal and cold temperatures beams. The cold resulted in an average stiffness increase of 18% under both static and dynamic conditions.

Further studies need to be completed to conclusively determine the effects of cold temperatures on glulam's stiffness under high strain-rate effects. Additional samples are required to confirm the results presented above. Additionally, tests at a wide variety of temperatures and cyclic temperatures should be considered. Lastly, considering specimens of other dimensions could improve the dataset and reliability of the effects reported in this study.

REFERENCES

[1] CSA. Design and assessment of buildings subjected to blast loads S850-12. CSA, Mississauga, ON, 2012.

[2] ASCE. Blast Protection of Buildings: ASCE/SEI 59-11 (Blast Protection of Buildings). 2011.

[3] K. A. Marchand. BAIT, BASS & RODS Testing Results. Applied Research Associates, Prepared for the USAF Force Protection Battlelab, 2002.

[4] D. Lacroix and G. Doudak. Determining the dynamic increase factor for glued-laminated timber beams. *Journal of Structural Engineering*, 144(9): 04018160-1 to 04018160-12, 2018.

[5] M. Poulin, C. Viau, D. N. Lacroix, and G. Doudak. Experimental and analytical investigation of cross-laminated timber panels subjected to out-of-plane blast loads. *Journal of Structural Engineering*, 144(2): 04017197-1 to 04017197-11, 2018.

[6] C. Viau and G. Doudak. Behaviour and retrofit options for light-frame wood stud walls subjected to blast loads. In: *Proceedings of the 11th International Conference on Shock and Impact Loads on Structures*, 2015.

[7] E. Jacques, A. Lloyd, A. Braimah, M. Saatcioglu, G. Doudak, and O. Abdelalim. Influence of high strain-rates on the dynamic flexural material properties of spruce–pine–fir wood studs. *Canadian Journal of Civil Engineering*, 41(1): 56-64, 2014.

[8] N. J. Parlin, W. G. Davids, E. Nagy, and T. Cummins. Dynamic response of lightweight wood-based

https://doi.org/10.52202/069179-0041

flexible wall panels to blast and impulse loading. *Construction and Building Materials*, 50: 237-245, 2014.

[9] D. Lacroix and G. Doudak. Investigation of Dynamic Increase Factors in Light-Frame Wood Stud Walls Subjected to Out-of-Plane Blast Loading. *Journal of Structural Engineering*, 141: 04014159-1 to 04014159-10, 2014.

[10] C. Viau. Investigation and Optimization of Connections in Timber Assemblies Subjected to Blast Loading. Doctor of Philosophy, Civil Engineering, Université d'Ottawa/University of Ottawa, 2020.

[11] C. Viau and G. Doudak. Energy-Absorbing Connection for Heavy-Timber Assemblies Subjected to Blast Loads–Concept Development and Application. *Journal of Structural Engineering*, 147(4): 04021027-1 to 04021027-13, 2021.

[12] A. McGrath and G. Doudak. Investigating the response of bolted timber connections subjected to blast loads. *Engineering Structures*, 236: 112112-1 to 112112-12, 2021.

[13] O. Stefanovich. Canada looks to reinforce Arctic sovereignty through diplomacy, military, says minister. In: CBC News, 2022.

[14] Government of Canada. Canadian Forces Station Alert. http://www.rcaf-arc.forces.gc.ca/en/alert.page (accessed 30 June 2021), 2021.

[15] X. Wang, J. Björnberg, O. Hagman, S. A. Ahmed, H. Wan, and P. Niemz. Effect of low temperatures on the block shear strength of norway spruce glulam joints. *BioResources*, 11(4): 9638-9648, 2016.

[16] G. Drake, M. Berry, and D. Schroeder. Effect of cold temperatures on the shear behavior of glued laminated beams. *Cold Regions Science and Technology*, 112: 45-50, 2015.

[17] R. Yang et al. Effects of Freeze-Thaw Cycles on Physical and Mechanical Properties of Glulam Exposed to Outdoor Environment. *Journal of Renewable Materials*, 9(7): 1293-1307, 2021.

[18] M. Beirnes, M.-A. Dagenais, and G. Wight. Cold temperature effects on the impact resistance of thin, lightweight UHPFRC panels. *International Journal of Impact Engineering*, 127: 110-121, 2019.

[19] N. Wight, C. Viau, and P. Heffernan. Behaviour and Resistance of Glued-Laminated Timber Subjected to Impact Loading. In: *Canadian Society for Civil Engineering Annual Conference*, Structural 149-1 to 149-10, 2022.

[20] ASTM International. Standard Test Methods of Static Tests of Lumber in Structural Sizes: D198 − 21a. ASTM International, Pennsylvania, United States, 2021.

[21] E. Karacabeyli and J. Barrett. Rate of loading effects on strength of lumber. *Forest Products Journal*, 43(5): 28-41, 1993.

[22] J. Biggs. Introduction to structural dynamics. McGraw-Hill College, 1964.

[23] D. N. Lacroix. Investigating the behaviour of glulam beams and columns subjected to simulated blast loading. Doctor of Philosophy, Civil Engineering, Université d'Ottawa/University of Ottawa, 2017.

[24] C. C. Gerhards. Effect of moisture content and temperature on the mechanical properties of wood: an analysis of immediate effects. *Wood and Fiber Science*, 14(1): 4-36, 1982.

[25] R. Schmidt and J. Pomeroy. Bending of a conifer branch at subfreezing temperatures: implications for snow interception. *Canadian Journal of Forest Research*, 20(8): 1251-1253, 1990.

[26] D. W. Green and J. W. Evans. The immediate effect of temperature on the modulus of elasticity of green and dry lumber. *Wood and Fiber Science*, 40(3): 374-383, 2008.

https://doi.org/10.52202/069179-0041